TEMPORAL EVOLUTION AND 3D LOCATIONS OF ACOUSTIC EMISSIONS PRODUCED FROM THE DRYING SHRINKAGE OF CONCRETE

GREGORY C. MCLASKEY and STEVEN D. GLASER
Department of Civil and Environmental Engineering, University of California, Berkeley, USA

Abstract

Acoustic emission activity produced by unrestrained drying shrinkage of an early age normal strength concrete specimen was measured with an array of fourteen broad-band high-fidelity acoustic emission sensors. The specimen was continuously monitored for 17 days, and full waveforms of the acoustic emissions were recorded throughout this time period. We present the source locations in three dimensions, the evolution of these events over time. Additionally, we discuss the reliability of source location estimates and consider uncertainty and bias introduced by array geometry effects, choice of velocity models, and poor picking of arrival times. We report on experimental procedures and tools created for fully quantitative, signal-based acoustic emission analysis.

Keywords: High fidelity, sensors, concrete, wave propagation, source location

Introduction

Drying shrinkage of concrete is a known cause of micro and macro cracking. Because the presence of cracks can have many detrimental effects on the durability of a concrete structure, it is important to understand the development of the cracks as the concrete ages. It is generally expected that shrinkage will commence almost immediately after exposure to a low relative humidity. Though aggregates complicate the stress state of a shrinking concrete specimen, cracking is expected to occur in the region of tensile stresses near the outside surface of the specimen [1].

Current research on drying shrinkage cracking in concrete relies on observations via optical microscopy [2]. These studies have confirmed that the location of drying shrinkage cracking is near the surface and around aggregates, and occurs during the first few days of drying. The disadvantage of these optical methods is that the specimen must be cut open. The method of acoustic emission allows cracks to be identified continuously and non-invasively.

In this paper, the cracking of concrete due to drying shrinkage without external restraint is studied through the method of acoustic emission. Similar experiments have been reported [3, 4] but for the first time the events are located in three dimensions and over a 17-day drying period. Additionally, the sources of error in the localization schemes are identified and quantified and error ellipsoids are calculated for each of the source location estimates.

Experimental Setup

A prismatic specimen (175 x 175 x 250 mm) of normal strength concrete with a water/cement ratio of 0.46, design strength of 27.5 MPa, and largest sized coarse aggregate of 15 mm diameter (pea gravel) was tested for drying shrinkage cracking using the method of acoustic emissions. The specimen was cast into a wooden mold with PMMA inserts for improved surface smoothness. The specimen was cured for 28 hours and then demoulded and instrumented with an array of NIST-Glaser-type high fidelity broadband transducers modeled after the NBS conical transducer [5]. The sensing element is PZT-5a (lead-zirconate-titanate) truncated cone with an

aperture diameter of 1.5 mm. The sensors have a very flat frequency response from 12 kHz to 960 kHz and with unidirectional sensitivity to particle displacement. Further details on the sensors can be found in [6, 7].

The prismatic specimen was instrumented with an array of fourteen sensors located on the North, East, South, and West sides of the specimen. (Sensor locations are shown in Fig. 2.) The top side of the specimen was exposed to ambient humidity (30±5% relative humidity) and the rest of the specimen was partially sealed with cellophane. Before digitization, all signals went through a DigitalWave™ FM-1 signal conditioner/preamplifier where they were subject to a gain of 36 dB and a 20 kHz high pass filter to remove low frequency background noise. The signals were sampled at 5 MHz using a 12-bit High-Techniques™ Digitizer. The specimen was continuously monitored for 17 days. During this time period if the voltage from any one of four preselected trigger sensors exceeded 31 mV (corresponding to displacements on the order of 3 pm), the digitizer was triggered and 800 μs of the displacement time history from each sensor was recorded and saved starting 250 μs before the time of triggering and ending 550 μs after the time of triggering. Each one of these triggered 'hits' was saved for offline analysis and was later classified either as an 'event' or as 'noise'.

Estimating the Location of Acoustic Emissions

Source location is perhaps the single most important analysis procedure in the method of acoustic emission because many other analyses—such as energy and magnitude estimates and source kinematics—rely on the accurate determination of the source location. There are a number of methods for determining a source location, but this paper will only discuss methods which use the observed arrival time of a specific wave phase at a number of sensor locations to calculate the coordinates of the source in space and time. (We refer to the wave phase as the P-wave because it is most commonly used. The same schemes could be implemented for S waves.)

Because the absolute source time is not known, finding source coordinates based on the differences in arrival times recorded from an array of n sensors requires the solution of a series of n-1 nonlinear equations. A solution (in the least squares or least error sense) can be found by calculating the minimum of a suitable cost function (usually iteratively). By subtracting one equation from the rest, the nonlinear equations can be manipulated into n-2 linear equations from which source coordinates can be solved directly; or, if more than five sensors are used, a method of 'quasi least squares" may be used [8, 9]. When errors are included in the arrival times, this method can produce wildly inaccurate results, thus it has been suggested that the 'quasi least squares' method be used only a starting point for an iterative scheme [10].

In our tests, the locations of the hypocenters of the acoustic emissions recorded were found using the minimization of the cost function

$$\text{cost} = \sum_{i=1}^{n} \left| \sqrt{(x - \mathrm{x}_i)^2 + (y - y_i)^2 + (z - z_i)^2} - c(t_i - t_0) \right| \qquad (1)$$

where t_i, x_i, y_i, and z_i are the observed P-wave arrival times, and the known spatial coordinates for the i^{th} sensor, c is the assumed wave velocity, n is the number of sensors used for the determination of the source location, and x, y, z, and t_0 are the unknown source location in three spatial dimensions and time. This method assumes (1) that the hypocenter and sensors can be modeled as points, (2) that the ray path from source to receiver is a straight line, and (3) that P waves travel at some known and constant velocity c.

Once an estimate of the source location is found, the quantification of uncertainty and bias in the source location estimate must be considered. In this study, the sources of errors were divided into four main categories: picking errors, array geometry-induced errors, velocity model errors,

and minimization errors. Note that all results presented here, both synthetic and real, are for the array and specimen geometry shown in Fig. 2.

Picking Errors

Picking errors are those which can be modeled by an inaccurate selection of the arrival time of the P-wave. Slow rise times or low signal to noise ratios can cause picking errors, but even if the arrival times are unambiguous, the observed arrival time may deviate from the ideal case. Equivalent picking errors may be calculated and quantified for these sources of error.

The majority of the events recorded from the drying shrinkage test have P-wave rise times of 1-3 μs which allow the arrivals to be picked to within an accuracy of about 500 ns. This provides a baseline from which other sources of picking error can be quantitatively compared. For example, the 1.5-mm aperture of the sensor would produce the equivalence of at most 170 ns of error for the P wave velocities found in concrete. (In contrast, an 8-mm diameter sensor aperture can produce up to 800 ns of equivalent picking error.) The increase in travel path due to a crack or void 3 mm in diameter would produce at most 80 ns of equivalent picking error under the geometry of our test setup. Alternatively, under the same geometry, if the average P-wave velocity deviates (due to inhomogeneities in the material, for example) from the assumed value by only 5% (200 m/s) it would produce 500 ns of equivalent error.

In order to model picking errors and gain an estimate of the uncertainty associated with each source location estimate, a random error term was added to each picked arrival time. This error term was assumed to be a normally distributed random variable with a mean of zero and a standard deviation of 500 ns. The source location was then calculated fifty different times, drawing upon fifty different realizations of the error terms. Error ellipsoids and confidence intervals were then calculated from the cluster of fifty source locations generated via this procedure.

Array Geometry Errors

While the array geometry does not introduce new errors, for certain source locations relative to the sensor array the picking errors can be amplified by array effects [10, 11]. This is similar to the concept of a blind spot in the sensor array. Figure 1(a) shows the effect of the sensor array and specimen geometry used for the drying shrinkage test setup. In the figure, the 95% confidence error ellipsoids are shown relative to the true location of simulated sources located on the top surface of the concrete specimen. The error ellipsoids are based on normally distributed random picking error with a mean of zero and a standard deviation of 500 ns. It was found that array geometry-induced errors are greatest near the corners of the specimen, especially the Southwest corner.

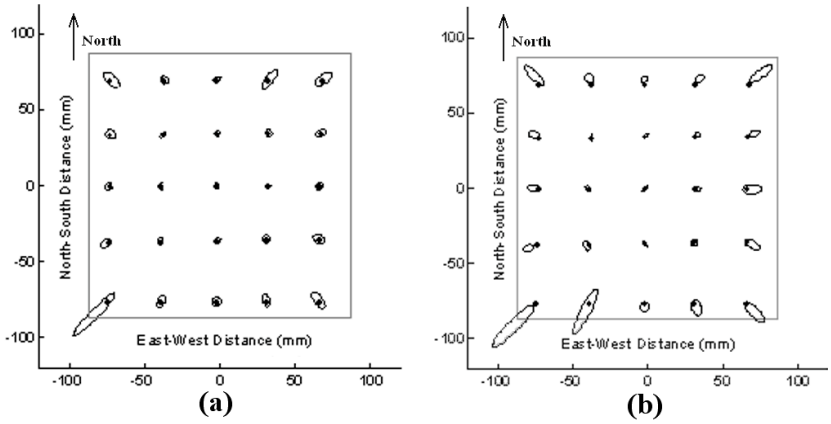

Fig. 1. Error ellipsoids for simulated sources located on the top surface of a specimen with identical array geometry to the drying shrinkage test setup demonstrate the amplification of picking errors due to (a) array geometry alone, and (b) bias induced by an inaccurate velocity model.

Velocity Model Errors

The cost function (1) used for localization assumes that the P-wave velocity is known and constant over every ray path in the concrete specimen, but in reality the P-wave velocity is unknown, difficult to measure, inhomogeneous, and is changing over time as the concrete cures and dries and cracks [12]. An incorrect velocity model will surely yield biased estimates of source location.

For example, if the assumed velocity is only off by 100 m/s (about 3%) the source location estimate will be biased by 1-4 mm depending on the true source location relative to the sensor array. Figure 1(b) shows the combined effect of picking errors (same as described above), array geometry, and velocity model errors (the assumed velocity is 100 m/s faster than the true velocity). This figure shows that this velocity model error will introduce uncertainty and will bias location estimates by pushing them further from the center of the sensor array.

Minimization Errors

Array geometry-induced errors, picking errors, and velocity model errors can yield cost functions which lack a well defined minima. Thus, a fourth category of errors can arise due to the imprecision and bias introduced by the algorithm which computes the minimization of the cost function. In the absence of errors, the cost function will vary smoothly over four dimensional space (three spatial dimensions and source time), but when deviations between observed and expected travel times are introduced, this function often becomes highly nonlinear. Iterative solution schemes often fail to find the global minimum and instead pick local minima or satisfy their convergence criteria on a very flat portion of their path, far from the true minimum. For this study, an iterative scheme which incorporates random jumps into the search path was used for the minimization of the cost function. While this solution strategy was computationally expensive, it was very robust and often performed better than conventional algorithms. By comparing different types of minimization schemes, imprecision was estimated to be on the order of 0.25-0.5 mm within the spatial region of interest.

Results and Discussion

Over two thousand acoustic emissions were recorded in the prismatic specimen over the 17-day monitoring period. About 800 events were deemed large enough to be located. Reasonably accurate (±10 mm) source locations were found for about 80% of those events. Figure 2 shows the principle axes of error ellipsoids for only those events which were found to be located near the center of the specimen (within the dashed lines) and with 95% confidence error ellipsoids less then 20 mm in all directions. (Error ellipsoids were found from the method described above.) Of these 340 events, most were located a few centimeters below the drying surface. A smaller number of events were found to be much deeper (8-10 cm) in the interior of the specimen.

The evolution of depth over the 17-day monitoring period (for the same 340 events shown in Fig. 2) is shown in Fig. 3. The bars represent 95% confidence intervals calculated via the same method as those shown in Fig. 2. The upper graph shows the locations found using a constant velocity model while the lower graph shows the results using a time varying velocity model. To estimate the change in P-wave velocity over time, pencil leads were broken at two different locations on the surface of the specimen on a daily basis, and from the evolution of pencil lead sources at known locations a velocity model was created which assumes that the P wave velocity is initially increasing and then leveling off over the 17-day period.

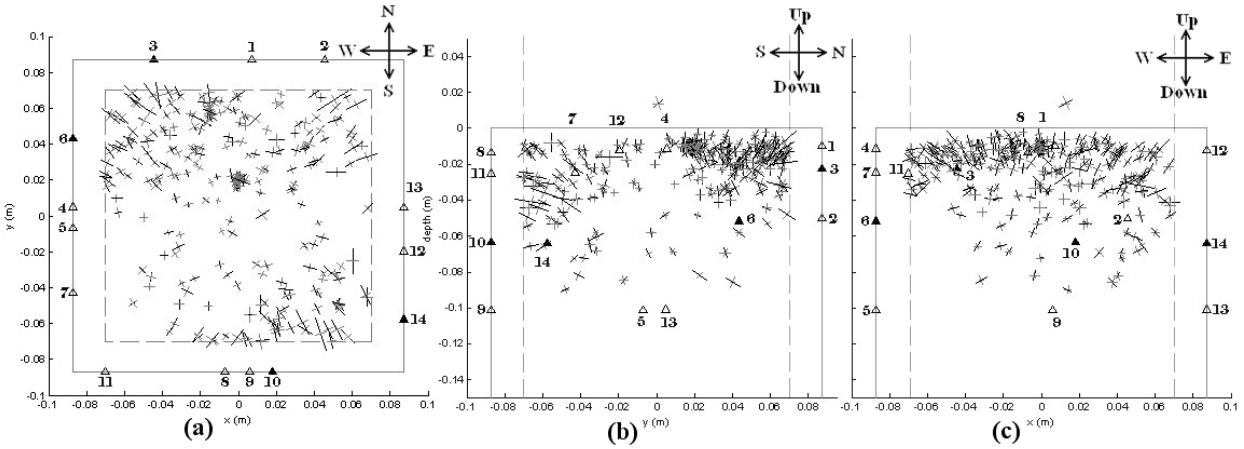

Fig. 2. Spatial distribution of estimated source locations in (a) top and (b, c) side views.

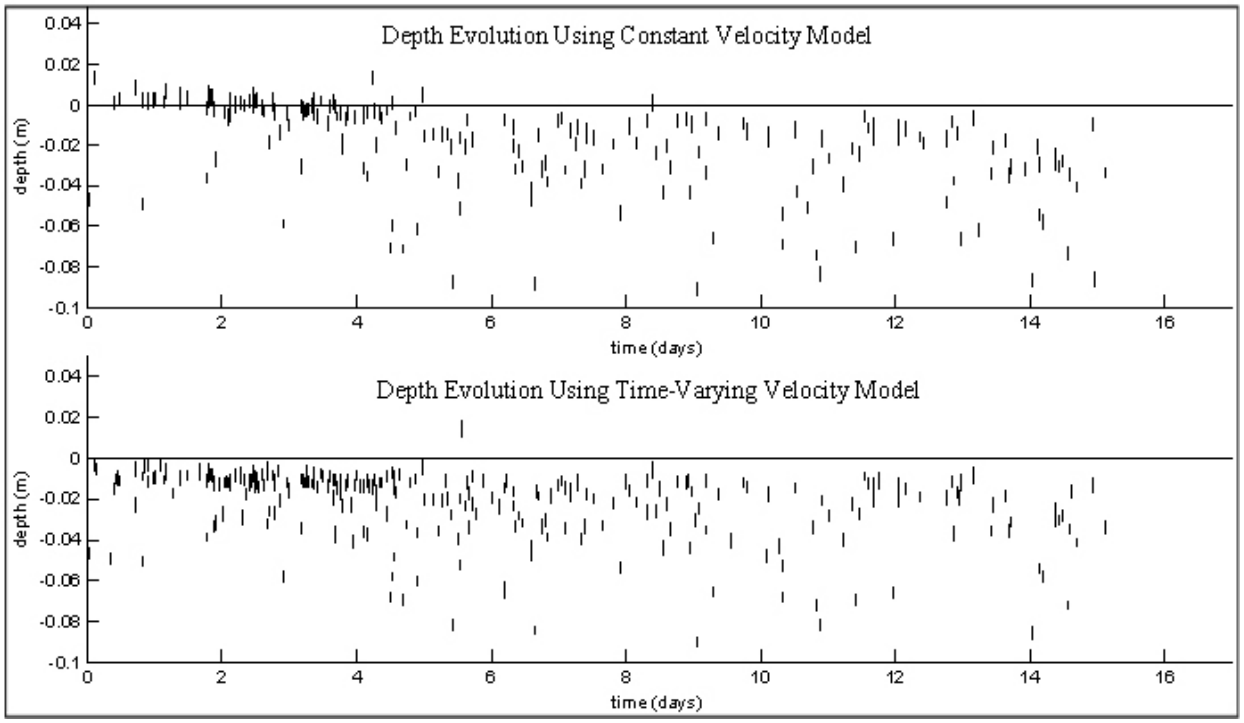

Fig. 3. Evolution of depth over time using (a) constant velocity model (b) time varying velocity model.

A very clear trend from surface to interior events can be seen from estimates using the constant velocity model, but the apparent increase in depth was due, in part, to bias induced by an inaccurate velocity model. For example, if the estimated velocity is higher than the true velocity, as is the case for the first few days of the monitoring period under the constant velocity model, the location will be pushed further from the center of the sensor array. In this case the inaccurate choice of velocity causes the events to locate above the surface of the specimen. From this analysis it is clear that the choice of velocity model can have a large effect on source location estimates, yet even with the time-varying velocity model a trend toward increasing depth is apparent.

One would expect that the emissions due to drying shrinkage would be spread evenly over the entire drying surface in plan view (Fig. 2(a)) and be located within a few centimeters of the surface in side view (Fig. 2(b) and (c)). The relatively small number of events found in the SW

corner of the specimen may be due to the large amount of array-induced localization errors in this location. The larger numbers of events in the NW and SE corners of the specimen may be due in part to a triggering bias (i.e. smaller events closer to trigger sensors are recorded while similar events further from trigger sensors will be undetected). The four trigger sensors (#3, 6, 10, 14) are shown as filled triangles in Fig. 2. Finally, while drying shrinkage cracking is expected to be located on or near the surface of the specimen, even under the time varying velocity model most events were estimated to be well beneath the surface of the specimen. This may be bias due to the inaccurate assumption of a homogeneous velocity model.

Despite the fact that inaccurate velocity assumptions make the absolute accuracy of source locations difficult to calculate, the relative uncertainty of the source locations is relatively well known, and the error bars shown in Figs. 2 and 3 provide a good measure of precision.

Conclusion

The 3D locations of hundreds of acoustic emissions recorded over a 17-day drying period have been estimated. Imprecision in P wave picking and the inhomogeneous nature of P wave velocity of concrete seem to be leading sources of picking errors. These picking errors may be amplified by the array geometry and minimization errors. By making use of equivalent picking errors, uncertainty was modeled, and the propagation of this uncertainty via array geometry effects and minimization errors can be accurately tracked. Alternatively, an inaccurate velocity model is a large source of error, and it is one that is very difficult to quantify. Consequently, the absolute accuracy of a source location is difficult to measure. Despite this, the relative precision of the estimates can be quantified and a clear trend from surface to interior events can be seen over the 17-day period in the drying concrete specimen.

References

1. Bisschop, J., *Drying Shrinkage Microcracking in Cement-Based Materials*, Delft University Press, 2002.
2. Bisschop, J., and van Mier, J. G. M., Materials and Structures, **35**, 2002, 453-461.
3. Shiotani, T., Bisschop, J., and van Mier, J. G. M. Engineering Fracture Mechanics, **70**, 2003, pp. 1509-1525.
4. Uomoto, T., Kato, H., *Progress in Acoustic Emission V*, eds. Yamaguchi, K., Takahashi, H., and Niitsuma, H., The Japanese Society for NDI, Sendai, Japan, 1990, pp. 325-330.
5. Proctor, T. M. Journal of Acoustic Society of America, **71**, 1982, 1163-1168.
6. Glaser, S., Weiss, G., and Johnson, L., Journal of Acoustic Society of America, **104**, 1998, 1404-1412.
7. McLaskey, G., Glaser, S., Grosse, C., Proc. of SPIE Vol. 6529, San Diego, Mar. 18-20, 2007.
8. Mahajan, A., and Walworth, M., IEEE Transactions on Robotics and Automation, **17**, 2001, 91-94.
9. Ohtsu, M., and Ono, K., NDT International, **21**, 1988, 143-150.
10. Salamon, M. D. G., and Wiebols, G. A., Rock Mechanics, **6**, 1974, 141-166.
11. Ge, M., and Hardy, H.R., *Fifth Conference on Acoustic Emission/Microseismic Activity in Geologic Structures and Materials*, Pennsylvania State University, June 11-13 1991.
12. Boyd, A. and Ferraro, C., ASCE J. of Materials in Civil Engineering, **17**, 2005, 153-158.